

Development of a laser-optical point sensor based on the Filtered Rayleigh Scattering technique for use under cryogenic conditions

Development of a laser optical point sensor based on the Filtered Rayleigh Scattering technique for use under cryogenic conditions

Ann-Katrin Hensch¹, Peter Guntermann¹, Michael Dues², Jonas Steinbock², Adi Siswanto², Guido Stockhausen³, Michael Fischer³, Eike Burow³, Manfred Beversdorff³

1) European Transonic Windtunnel GmbH, 51147 Cologne, Germany

2) ILA R&D GmbH, 52428 Jülich, Germany

3) Institute of Propulsion Technology (AT), DLR, 51147 Cologne, Germany

Keywords: Filtered Rayleigh Scattering, FRS, LDV, contactless freestream sensor
Key words: Filtered Rayleigh Scattering, contactless freestream sensor, FRS

Summary

This publication describes the development and testing of a non-contact flow sensor based on the Filtered Rayleigh Scattering principle for use in the European Transonic Windtunnel (ETW) under cryogenic conditions. The required sensor was developed in several steps and tested under cryogenic conditions in the wind tunnel. The innovative approach consists of the combination of cryogenic-compatible, non-intrusive endoscopic hardware with fast data acquisition at a constant laser frequency in order to convert the already developed and successfully tested slow frequency scanning method for stationary planar measurements into a transient point measurement method.

Introduction

When carrying out aerodynamic investigations in the European Transonic Windtunnel (ETW) under cryogenic conditions, the reproducible setting of the operating point and precise knowledge of the velocity of the core flow in the measurement chamber or at other reference points is of great importance for the comparability of measurements. Until now, total pressure probes and static pressure probes have been used for these purposes, which are regularly calibrated and compared with reference measurements. Other probes, such as hot-wire anemometers, can be used for measurement, but represent an intrusive measurement method and their operation under cryogenic conditions is associated with comparatively high costs. The latter are unsuitable as a permanent measuring device in the wind tunnel, as they are very sensitive and are exposed to high mechanical loads. The aim of a joint research project between ETW, DLR and ILA R&D GmbH is therefore to develop a laser-optical sensor for the precise recording of flow parameters, which also does not require the addition of seeding particles. In the LuFo V-3 project entitled OFRS (Optical Flow Sensor for Cryogenic Conditions based on FRS), a point sensor based on filtered Rayleigh scattering technology is to be developed that also offers the potential for time-resolved transient measurements. To this end, tests were carried out in the Pilot European Transonic Windtunnel (PETW), the results of which are shown in this publication. The tests were carried out with sensors in various stages of development.

Measuring environment Pilot European Transonic Windtunnel (PETW)

The sensor was tested in the Pilot European Transonic Windtunnel (PETW), which is the pilot facility of the ETW and was built to pre-test and validate cryogenic wind tunnel technology before the ETW was designed and built. To this day, the PETW is still used as a test facility to qualify new measurement methods or hardware components under cryogenic conditions. The PETW is a version of the ETW scaled by a factor of 1:8.8 and allows identical operating points (pressure, temperature, speed) to be set. It is a wind tunnel of Göttingen design that achieves characteristic Reynolds numbers of transport aircraft by increasing the pressure (125 kPa to 450 kPa) and lowering the temperature by injecting liquid nitrogen (300 K to 115 K), see Fig. 1 (left). The resulting high (molecular) density is a decisive advantage when using FRS as a measuring method or flow sensor.

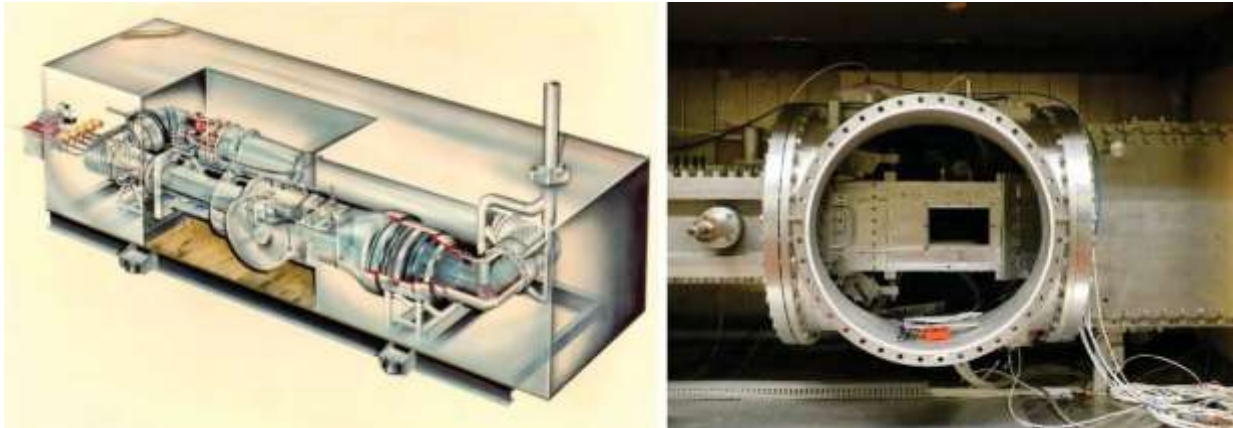


Fig. 1: Diagram of the PETW flow circuit. View into the measuring section of the PETW

The measuring section of the PETW has dimensions of 0.229 m x 0.271 m (height x width) with slotted ceiling and floor walls. Optical access to the PETW measuring section is possible through a rectangular window installed in the side wall (see Fig. 1) and two portholes in the flange of the pressurised enclosure (not shown here). The plenum and outer insulation of the PETW differ from those in the ETW, which proved to be disadvantageous for the measurements described here with regard to optical access compared to a potential application in the ETW, but nevertheless allowed a "proof-of-principle".

FSM-FRS measuring principle

The FRS method is based on analysing the Rayleigh scattering of the laser light on the gas molecules in the flow. The Rayleigh scattering occurring at the gas molecules has a spectral distribution of several GHz width and contains information about temperature, pressure, velocity and density in the illuminated measuring range. However, reflections of laser light on walls (geometric scattering) or particles (Mie scattering) are not broadened in frequency and can be filtered out of the measurement signal with the aid of a molecular filter, in this case an iodine cell. Fig. 2 shows the formation of the FRS spectrum.

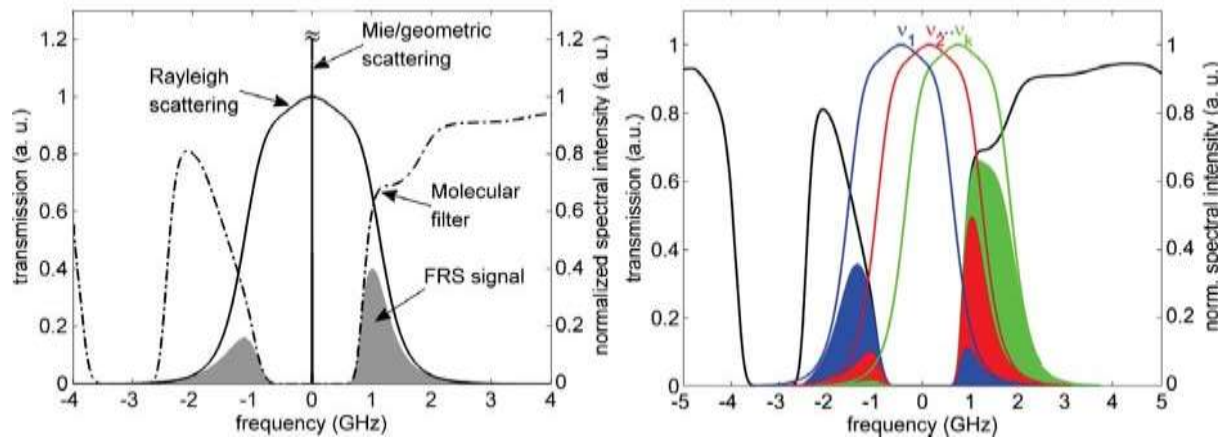


Fig. 2: From Doll et al. (2014): Narrow-band laser light is Rayleigh scattered at the fluid molecules and filtered with an iodine cell, removing reflections from surfaces and scattering from large particles (Mie scattering). (right) Frequency scan method: The laser frequency is shifted along the transmission profile of the molecular filter. Time-averaged pressure, temperature and velocity fields (Doppler shift) can be determined simultaneously from the resulting intensity spectra. Fig. 9 shows an example of the resulting intensity spectra.

The light scattered by the molecules is imaged through the iodine cell onto a photomultiplier and transferred into an intensity value. However, the spectral information on temperature, pressure, density and speed is lost as a result. According to the frequency scan FRS method (FSM-FRS) further developed by DLR Cologne, the frequency of the laser system is therefore varied in discrete steps along the filter curve of the iodine cell, so that an intensity curve is created depending on the laser frequency. The temperature, pressure, velocity and density can be reconstructed from this intensity curve using a suitable measurement model, see Dues et al. (2018).

ILA FRS Sensor / DLR FRS Sensor

In this research project, two different FRS-based point sensors are being developed. The DLR sensor will be optimised in terms of signal quality and therefore designed with the largest possible apertures. This will allow the possibilities and limits of the technology to be tested. Based on DLR's experience, the ILA sensor will be designed in such a way that the sensor can also be installed later in the ETW under very limited space conditions. This requires a significant reduction in the size of the sensor, which is, however, associated with a deterioration in the signal-to-noise ratio. The extent to which this ILA probe still has sufficient signal quality for measurements under cryogenic conditions will be tested in a proof-of-principle test in the PETW. Due to the limited availability of the PETW and the relatively high operating costs, the measurement uncertainty will be analysed in detail on an ILA test bench.

In the first stage of development, both the DLR sensor and the ILA sensor are set up with a central signal generating laser beam and its focus is imaged backwards onto a photomultiplier located in the probe. The measurement volume is therefore formed by superimposing the laser focus with its image on a pinhole in front of the detector. Both sensors work with a polarisation-maintaining PCF fibre to transmit the laser light to the probe. The laser used is a fibre laser from the manufacturer Azurlight Systems (5 W, 532.3 nm) in conjunction with an NKT seeding laser. The laser is characterised by a relatively small spectral width of less than 200 kHz and a wide adjustment range. By controlling the seeding laser, the frequency of the fibre laser can be shifted in the range of 10 GHz. The wavelength of the fibre laser is measured with a wavelength meter which/that is calibrated by a frequency stabilised HeNe laser and controlled with a control output to the seeding laser.

Experimental setup and proof-of-principle at PETW

The PETW was used to qualify the sensors in the "empty measuring section" configuration so that the point measurement of the flow parameters can be carried out by the sensor in the core flow of the measuring chamber. In the side wall of the measuring section, as well as in the porthole of the pressure hull, glass panes with an anti-reflective coating in the range of 532 nm for laser transmission angles of 0-30° were installed especially for the FRS measurement technology. This is of great importance, as different angles of the sensor's transmitter unit were tested in the wind tunnel tests in order to be able to determine the influence of the flow velocity on the measurement signal to varying degrees. The transmitter and receiver units of both sensors were integrated into a heated housing for all tests at the PETW so that the sensor was positioned as close as possible to the measurement location. Fig. 3 (left) shows the housing of the FRS probe in the PETW. Fig. 3 (right) shows the installation configuration for 0 degrees.

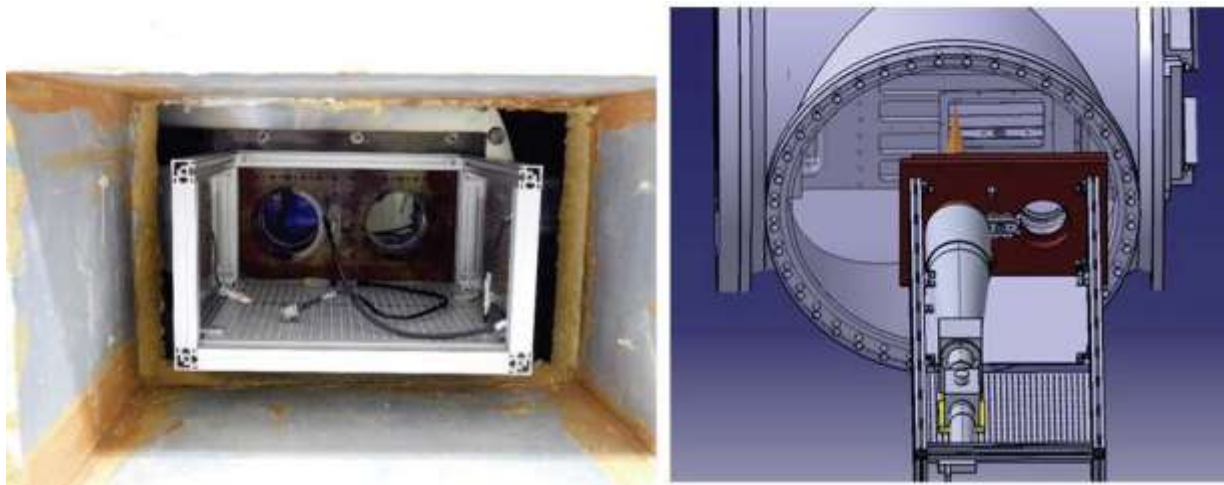


Fig. 3: Heated environment for sensor installation (left). Positioning the probe below 0 degrees (right).

The tests were carried out for two configurations. Firstly, the FRS signal was calibrated in the plenum of the PETW at known temperature (275 K - 115 K) and pressure conditions (150 kPa - 390 kPa) without flow. For this purpose, the focus of the sensor was moved into the plenum in the area between the measuring section and the heated housing. The measurements were then carried out in the measuring section under different flow conditions and sensor angles. Velocities of $Ma=0.3$ to 0.6 were set in the measuring section at temperatures of 250 K to 120 K and varying static pressure of 150 kPa to 250 kPa.

Fig. 4, shows the installation of the DLR and ILA sensor on the PETW. With the DLR sensor, deviations from the speed measured by the ETW of 4-7 % could be realised for different speeds. The deviation in the static temperature was 2-3 %, whereby it should be noted that the static temperature was determined in the plenum of the PETW and not in the FRS measuring plane.

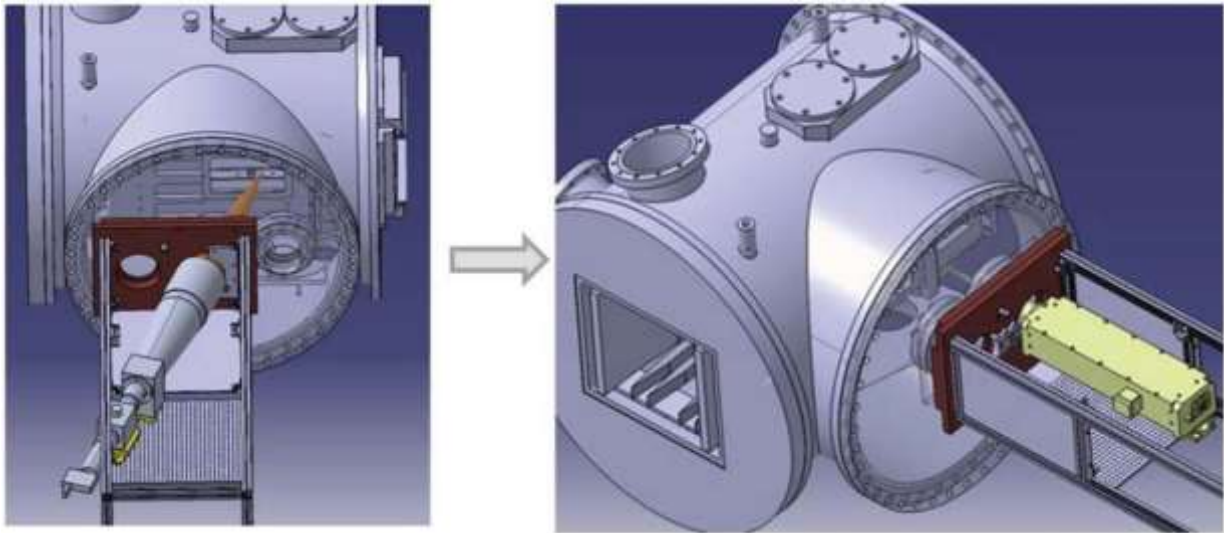


Fig. 4: Installation of the DLR sensor on the PETW at an angle of about 20°, and installation of the smaller ILA sensor on the PETW.

Compared to the values determined by the ETW, the ILA sensor achieved a deviation of 3.6 % on average with a spread of 3 %.

This means that both sensors have demonstrated their functionality under cryogenic conditions in the PETW proof-of-principle test. However, the measurements also show that there is still room for optimisation for both sensors, which is explained below.

Further development of the OFRS probes of DLR and ILA

The DLR sensor was extended with a second detector which, in addition to the FRS signal filtered in the iodine cell, also measures the intensity in front of the iodine cell. This signal can then be used for normalisation on the one hand and for measuring the density on the other, see Fig. 6.

With regard to the ILA probe, it became apparent that although the probe is fundamentally suitable for measurements under cryogenic conditions, it still requires too much installation space for later integration into the large ETW channel. For this reason, a fundamentally new concept was implemented that deviated from the previous DLR methodology. The starting point for the new ILA-OFRS probe was the classic design of an unshifted LDV probe, which was extended with a polariser and a reference measurement of the laser power. The OFRS signal now comes from the intersection of the two crossed laser beams, the LDV measurement volume, which is imaged onto a multimode optical fibre. The OFRS signal is transmitted through the fibre to the iodine cell located outside the probe, see Fig. 5.

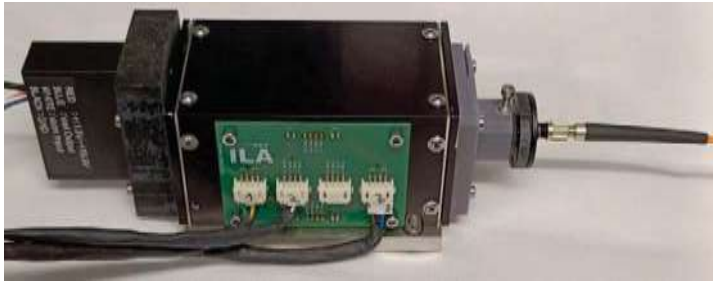


Fig. 5: Temperature-stabilised iodine cell with optical fibre connection and photomultiplier.

This new structure offers the following advantages:

By relocating the iodine cell outside the probe, it can be significantly reduced in size. This also makes the probe significantly less sensitive to the strong temperature fluctuations that are to be expected in the cryogenic wind tunnel despite temperature-controlled housings.

The spatial resolution can be significantly improved from approx. 30 mm to 3.2 mm by reducing the measuring volume at the intersection of the LDV beams. The measuring volume is defined here as the area in which the laser power has dropped to $1/e^2$.

Without modifying the probe, the OFRS measurements can be calibrated with an accurate and traceable LDV measurement in the same setup by briefly adding seeding. This means that the measurement is independent of the measurement accuracy of the sensors installed in the wind tunnel.

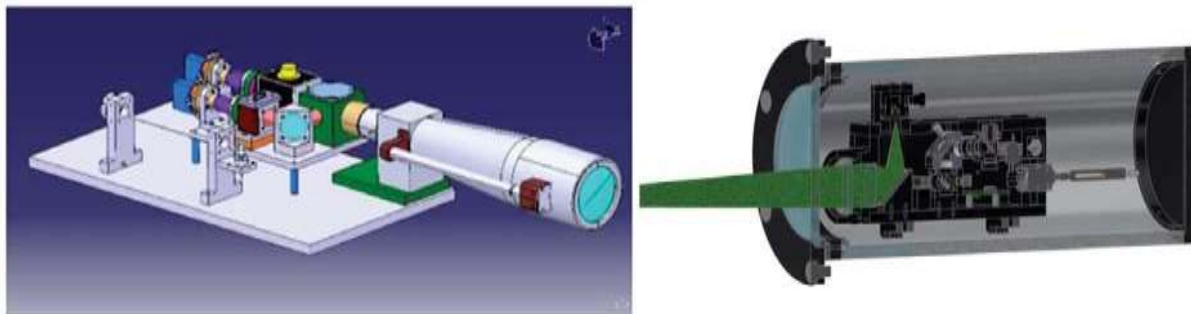


Fig. 6: Optimization of the DLR sensor with an additional detector (left), installation of the combined LDV/OFRS probe in the temperature-stabilised housing of the ETW (right).

The measurement uncertainty of the new ILA-OFRS sensor was analysed on an ILA test bench at ambient temperatures, as the PETW is only available for a very limited time due to operational reasons and incurs relatively high operating costs. As the amplitude of the FRS signal is proportional to the pressure, a significantly higher signal strength can be assumed in the ETW channel, as this is operated at up to 4.5 bar.

Measuring environment ILA test bench

The simplified test setup (Fig. 7) essentially consists of a conditioned pipe flow (pipe inner diameter 80 mm, see Fig. 8 above) in whose measuring cross-section flow velocities of approx. 30 to 100 m/s can be generated. Optical access is via an anti-reflective glass tube.

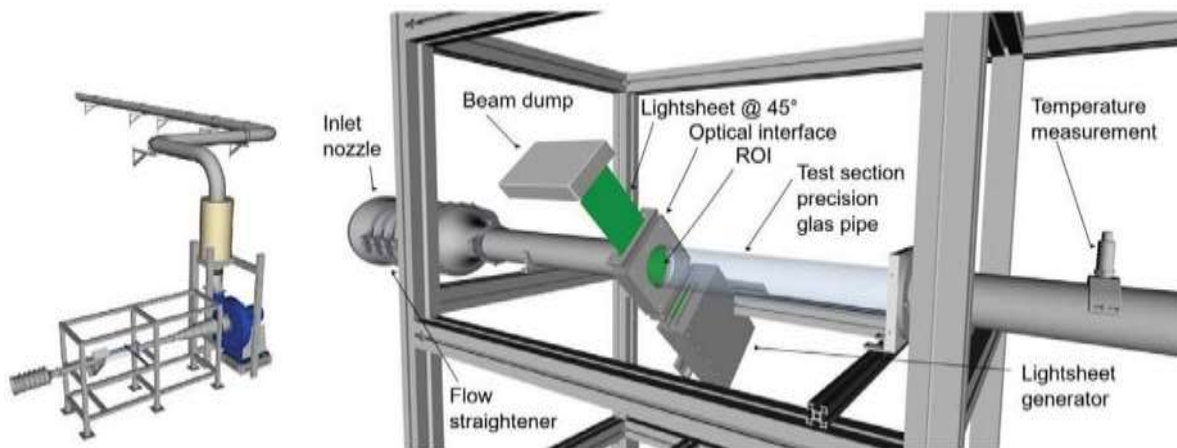


Fig. 7: Test rig for analysing pipe flows.

Due to the flow straightener, the contraction of the flow in the inlet nozzle and the relatively short distance to the measuring cross-section, a fully developed pipe flow profile is not expected there.

To characterise the test stand, network measurements were carried out at three different operating points using a calibrated LDV system. As the standardised flow profile does not change for these operating points, the volume flow can be carried out via a point measurement in the centre of the pipe and additionally a calibration of the differential pressure measurement at the measuring nozzle, see Dues et al. (2023). Above all, the flat flow profile in the centre of the pipe means that the velocity profile there is locally constant. Therefore, there are hardly any error influences due to deviations in the positioning of the OFRS probe, see Fig. 8.

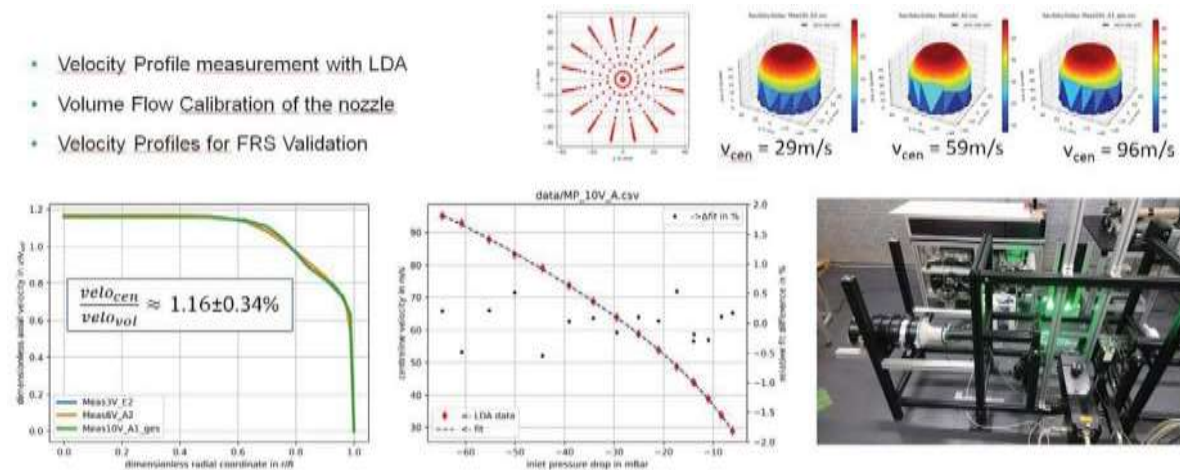


Fig. 8: Characterisation of the test rig with regard to velocity profile and pressure loss at the inlet nozzle for various operating points.

Investigation of measurement uncertainty on the ILA test bench

The movement of a molecule results in a Doppler shift of the Rayleigh signal in the FRS measurement. The Doppler shift is proportional to the velocity and the projection of the velocity vector onto the difference between the observation and laser vectors. The geometric arrangement is therefore taken into account to recalculate the velocity from the Doppler shift. In the present case of a conditioned nozzle flow, only the axial flow component is determined.

To determine the effective alignment of the OFRS probe to the longitudinal axis of the pipe, the probe is first positioned at a 90° angle to the pipe on the ILA test stand. The measuring volume is positioned in the centre of the cross-section, with the LDV probe recording the axial velocity component. The test stand is operated at different velocities, the centre velocity (LDV) and the pressure drop at the inlet nozzle are recorded. As the FRS optics cannot detect a Doppler shift at 90° , a measurement must be taken at an inclination angle to the main axis of the pipe to determine the axial flow component. In this case, the probe is mounted at an angle ($\sim 45^\circ$) to the longitudinal axis, with the measuring volume remaining in the same radial position. The LDA velocity now measured can be converted into the 90° measurement via the angle of rotation, provided that the same pressure loss occurs at the inlet nozzle. To determine the effective angle of rotation, 14 operating points are recorded in each case and the total difference between the converted velocities is minimised by varying the assumed angle of rotation. The calculated inclination angle is 46.4° .

The measurements at 27 m/s were excluded from the evaluation as, due to the open design of the test rig, it cannot be ruled out that external influences (wind) have an effect on the displayed pressure loss of the inlet nozzle during these measurements. The remaining 7 measurements, each with 5 repetitions, were analysed. Fig. 9 shows the resulting FRS spectra for one measurement as an example.

For the measurements on the laboratory test bench (ILA), an average deviation of 0.45 m/s or 0.7 % for the velocities results after taking a static velocity offset into account, see Table 1. The previously performed LDV measurements serve as a reference; the uncertainty is estimated to be $< 1\%$ for the velocity reference. The static offset for the axial velocity is approx. 9 m/s and can be justified with the absolute uncertainty of the frequency measurement. The corresponding frequency shift of 2.3 MHz is within the maximum frequency deviation of 10 MHz of the wavelength measuring device (HighFinesse WS). The maximum deviation of the velocity determined in this way is 0.8 m/s or 1.35 %. The standard deviation for determining the speed in a repeat measurement is less than 2 % in all cases.

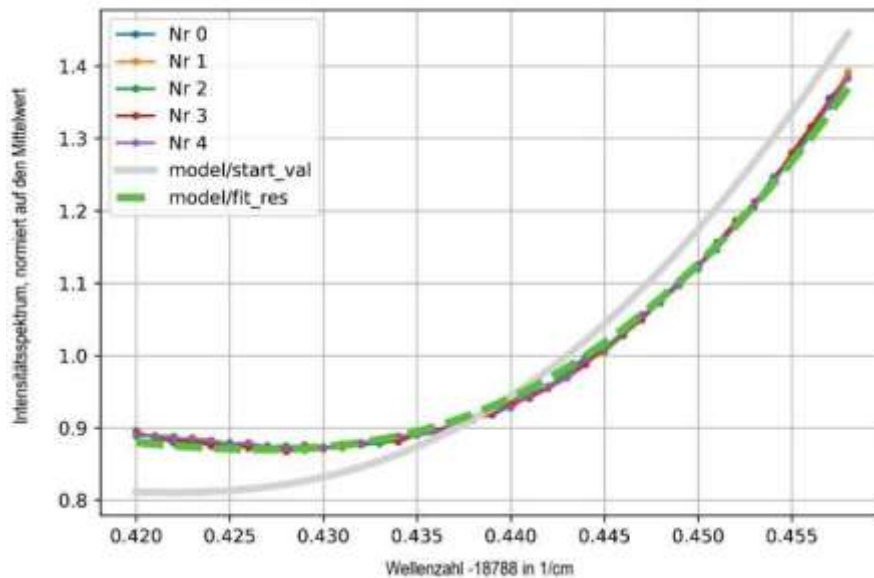


Fig. 9: Measured and fitted FRS spectra, after normalisation to the mean intensity value of the wavenumber range shown. No. 0 to 4 measured values for 5 frequency scans at a nominal velocity of approx. 70 m/s; the ML- RBS model (Melnikov et al. (2023)) and the convolution with the calibrated iodine line are taken into account for the calculated spectra. Grey continuous line: start spectrum for the adjustment calculation with the model; dashed green line: resulting intensity spectrum after the fit.

Measurement	Ref.Velocity[m/s]	FRS.Velocity[m/s]	Dev.[m/s]	Dev.[%]
4V	37,49	37,84	0,35	0,94
5V	48,14	47,49	0,65	1,35
6V	58,99	58,84	0,15	0,25
7V	69,59	68,82	0,77	1,10
8V	79,57	79,57	0,00	0,00
9V	88,77	89,57	0,80	0,90
10V	96,39	96,80	0,41	0,43
		Mean Value	0,45	0,71
		Standarddeviation	0,28	0,45

Tab. 1: Measurement deviation of the FRS system on the ILA test bench. The LDV measurements at 90° serve as a reference. The "Measurement" column contains the control voltage that is nominally applied to the frequency converter of the fan to set a desired speed.

Time-resolved FRS measurement of the DLR with the F0 method

The "f0" method is one way of measuring with a temporal resolution of 0.1-1 kHz. Here, the frequency of the laser is stabilised at the edge of an absorption minimum and only the amplitude value of the spectrum at this frequency is determined. This method can be used to record the fluctuations in speed, temperature and pressure, but the measurement uncertainty achieved is not yet sufficient for an absolute determination of the measured variables. This measurement method has already been successfully trialled in test measurements in the PETW.

For this purpose, the speed in the PETW was varied in the form of a ramp. However, the duct pressure could not be kept constant. Fig. 10 shows the variation of the measured velocity and the measured static pressure. The FRS f0 signal clearly follows the change in velocity, but also shows deviations due to the simultaneous change in static pressure. This influence can be eliminated by simply normalising the FRS f0 signal with a factor for the static pressure.

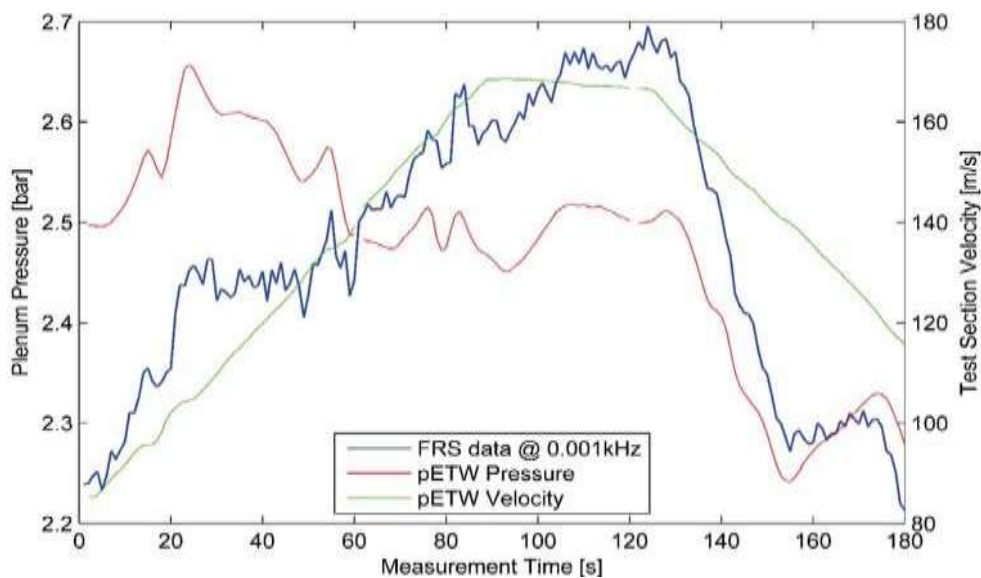


Fig. 10: FRS measurement using the f0 method with variable velocity and associated pressure change in the PETW channel

Fig. 11 shows that the FRS-f0 signal clearly follows the change in velocity in the signal. A future normalisation of the signal to the unfiltered Rayleigh intensity, which is proportional to the density that can be detected with a second photo detector, is expected to significantly improve the measurement deviation.

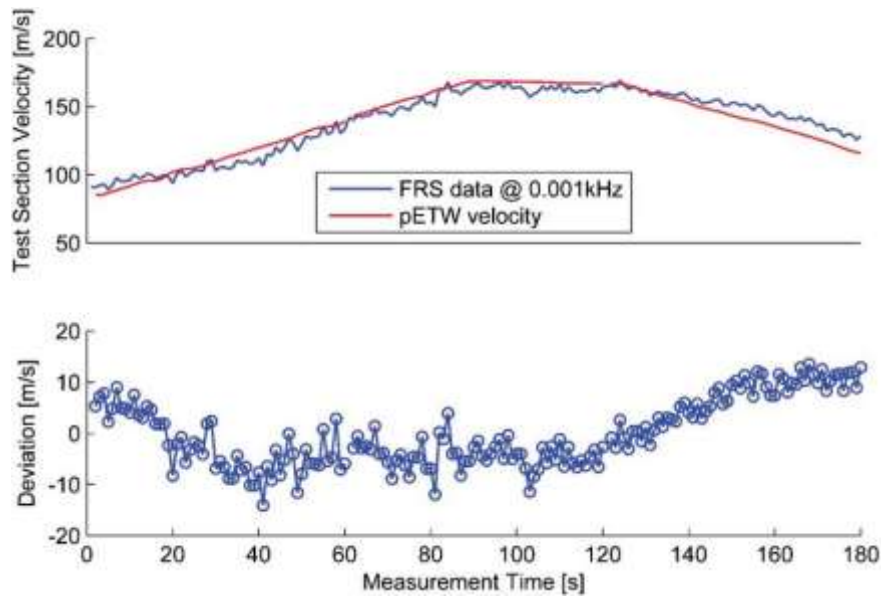


Fig. 11: FRS- f_0 signal, normalised to the static pressure and averaged to 1Hz, so that a comparison with the PETW pressure sensor is possible

Summary and outlook

In the project presented, a point sensor was developed which, in principle, enables the simultaneous detection of speed, temperature and pressure with a temporal resolution of a few Hertz. The sensor was developed for use under cryogenic conditions and works without the addition of seeding. The suitability for use under cryogenic conditions was proven by measurements in the Pilot European Transonic Windtunnel (PETW). Because LDV measurements can also be performed with the developed optics without system conversion, a traceable calibration of the FRS sensor in the installed state with short-term particle addition is possible. An average absolute deviation of < 0.5 m/s was demonstrated for the FRS system compared to the LDV reference measurements.

The sensor is now available for use in wind tunnels, especially in applications where seeding the flow with particles is difficult or undesirable. This is certainly the case with cryogenic tunnels or transonic wind tunnels.

Acknowledgements

The authors would like to thank the Federal Ministry of Economics and Climate Protection (BMWK) for funding the LuFo V-3 project "OFRS" with the funding code 20Q1729B. The authors would also like to thank the colleagues involved from the Institute of Propulsion Technology, ILA R&D and ETW, without whom it would not have been possible to carry out the measurement and record the corresponding results.

Literature

Doll, U., G. Stockhausen, and C. Willert. 2014. "Endoscopic filtered Rayleigh scattering for the analysis of ducted gas flows". *Experiments in Fluids*, 3 (55). <https://doi.org/10.1007/s00348-014-1690-z>.

Dues, M., U. Doll, T. Bacci, A. Picchi, G. Stockhausen, and C. Willert. 2018. "Laser-optical investigation of the flow field behind the turbine grid of a simulation test rig using Filtered Rayleigh Scattering". *Symposium "Experimental Fluid Mechanics"*.

Dues, M., J. Steinbock, U. Doll, I. Röhle, S. Melnikov, P. Zachos, and M. Migliorini. 2023. "Planar seeding free measurement of time-averaged 2D3C velocity, pressure and temperature fields using the Filtered Rayleigh Scattering method". *Symposium "Laser Methods in Fluid Dynamics"*.

Melnikov, S., I. Röhle, U. Doll, M. Dues, J. Steinbock, M. Migliorini, and P. Zachos. 2023. " Machine learning approach for fast evaluation of filtered Rayleigh scattering measurement data ". *Symposium "Laser methods in flow measurement technology"*.